Marine Geology 211 (2004) 169–187

MARINE GEOLOGY
INTERNATIONAL JOURNAL OF MARINE GEOLOGY, GEOCHEMISTRY AND GEOPHYSICS

www.elsevier.com/locate/margeo

# Estimating suspended solids concentrations from backscatter intensity measured by acoustic Doppler current profiler in San Francisco Bay, California

Jeffrey W. Gartner

*U.S. Geological Survey, Water Resources Division, Menlo Park, CA, USA*

Received 29 July 2003; received in revised form 2 June 2004; accepted 2 July 2004

**Abstract**

The estimation of mass concentration of suspended solids is one of the properties needed to understand the characteristics of sediment transport in bays and estuaries. However, useful measurements or estimates of this property are often problematic when employing the usual methods of determination from collected water samples or optical sensors. Analysis of water samples tends to undersample the highly variable character of suspended solids, and optical sensors often become useless from biological fouling in highly productive regions. Acoustic sensors, such as acoustic Doppler current profilers that are now routinely used to measure water velocity, have been shown to hold promise as a means of quantitatively estimating suspended solids from acoustic backscatter intensity, a parameter used in velocity measurement. To further evaluate application of this technique using commercially available instruments, profiles of suspended solids concentrations are estimated from acoustic backscatter intensity recorded by 1200- and 2400-kHz broadband acoustic Doppler current profilers located at two sites in San Francisco Bay, California. ADCP backscatter intensity is calibrated using optical backscatterance data from an instrument located at a depth close to the ADCP transducers. In addition to losses from spherical spreading and water absorption, calculations of acoustic transmission losses account for attenuation from suspended sediment and correction for nonspherical spreading in the near field of the acoustic transducer. Acoustic estimates of suspended solids consisting of cohesive and noncohesive sediments are found to agree within about 8–10% (of the total range of concentration) to those values estimated by a second optical backscatterance sensor located at a depth further from the ADCP transducers. The success of this approach using commercially available Doppler profilers provides promise that this technique might be appropriate and useful under certain conditions in spite of some theoretical limitations of the method.


*Keywords:* suspended solids concentration; acoustic backscatter intensity; acoustic Doppler current profiler; San Francisco Bay, California

*E-mail address:* jgartner@usgs.gov.

0025-3227/$ - see front matter © 2004 Elsevier B.V. All rights reserved.
doi:10.1016/j.margeo.2004.07.001

## 1. Introduction

Suspension, transport, and deposition of sediments in bays and estuaries are processes of critical importance to understanding the overall condition of these complex and often highly variable marine systems. In addition to providing habitat for benthic organisms, bottom sediments are a source of nutrients as well as potentially toxic materials such as pesticides and metals that readily adsorb to sediment particles (Hammond et al., 1985; Kuwabara et al., 1989). Transport of suspended sediments has the potential to distribute these materials within the system. Suspended sediments affect photosynthesis by limiting light transmission, and the deposition of sediments in shipping channels requires periodic dredging to maintain those channels in navigable condition (Buchanan and Schoellhamer, 1999).

Knowledge of mass concentration of suspended solids (SSC) is necessary to understand these sediment transport processes; however, measurement of this potentially rapidly fluctuating property has always been difficult at best. The primary traditional measurement technique has been to take periodic water samples for later analysis. This method may be adequate for some applications but has limitations especially when used in bays and estuaries because of the changeable character of suspended materials. Even collecting frequent water samples cannot accurately define a time series of suspended material that is often highly (spatially and temporally) variable and is modified by tidal currents, water depth, and wind effects.

Use of in situ optical instruments such as optical backscatterance (OBS) sensors (Downing et al., 1981; Downing, 1983) and transmissometers with the capability of producing time series of high-frequency measurements of suspended material help address the variable nature of SSC. However, calibration of these instruments is complicated because the response function of the OBS sensor depends on grain size and is nonlinear with concentration (Downing, 1996). In addition, optical sensors are extremely sensitive to biological fouling problems (Hamilton et al., 1998). Often, only a few days of data are usable from records collected in highly productive estuaries unless optical sensors are frequently cleaned.

Alternatively, acoustic sensors that are far less susceptible to effects of biological fouling (Downing, 1996) have shown promise for determining reliable estimates of suspended solids (e.g., Thorne et al., 1991; Hay and Sheng, 1992; Osborne et al., 1994). Thevenot and Kraus (1993) and Hamilton et al. (1998) provide extensive comparisons of the strengths and weaknesses of optical and acoustic methods for monitoring suspended materials. While many early studies primarily dealt with suspensions of sand-size material, some later studies (e.g., Hamilton et al., 1998; Jay et al., 1999) examine the potential for determining suspended cohesive sediment concentration.

As use of acoustic Doppler current profilers (ADCPs) has become more widespread, so have attempts to characterize suspended material from acoustic backscatter intensity measurements made by those acoustic instruments used to measure water velocity (e.g., Thevenot et al., 1992; Reichel and Nachtnebel, 1994). In addition to being less susceptible to biological fouling, commercially available ADCPs may provide nonintrusive estimates of SSC profiles concurrent with measurements of velocity profiles using the same instrument. However, the process of converting backscatter intensity to mass concentration is not straightforward. Among other things, complex acoustic transmission losses from beam spreading and attenuation must be accounted for correctly. They depend on multiple factors including environmental characteristics such as suspended material and the salinity, temperature, and pressure (of the water), and instrument characteristics such as power, transducer size, and frequency. While most early studies utilizing acoustic backscatter to estimate suspended solids typically include beam spreading and (water) absorption in the calculation of acoustic transmission losses, they often omit corrections for attenuation from suspended particles and nonspherical spreading in the transducer near field. More recent studies have begun to include these factors into consideration.

Jay et al. (1999) apply a correction function for improved calculation of beam spreading losses in the ADCP transducer near field to account for the complex acoustic beam pattern, and Holdaway et al. (1999) account for sediment attenuation in their evaluation of ADCPs to estimate suspended sediment concentration. Land and Jones (2001) describe Sediview, their commercially available software for estimating suspended sediment. Corrections are applied within Sediview for scattering by suspended material in the acoustic path and Land and Jones (2001) describe their intention to incorporate a two-stage correction for beam spreading in the next version of the Sediview software (now available). Hill et al. (2003) apply both corrections for attenuation from sediment and near-field spreading. However, with the exception of the work by Jay et al. (1999) and Holdaway et al. (1999), these studies describe only short-term estimates of SSC. There is a deficiency of published reports that describe the estimation of SSC over multiple tidal cycles using commercially available ADCPs that account both for attenuation from suspended material and corrections to near-field acoustic spreading in their treatment of acoustic transmission losses.

The objective of this paper is to investigate the suitability of using commercially available ADCPs to provide time series of profiles of SSC over multiple tidal cycles in an estuarine environment in which suspended material consists of cohesive and non-cohesive sediments. A field experiment in San Francisco Bay, California, is described in which time series of SSC are estimated from profiles of acoustic backscatter intensity measured by RD Instruments[1] 1200 and 2400 kHz BB-ADCPs at two locations over a 10-day period. (The term ADCP now refers to this entire class of instruments regardless of manufacturer; however, RD Instruments manufactured instruments that were used in the present study.) A short discussion of the theoretical background of the technique, including corrections for attenuation from suspended materials and nonspherical spreading in the transducer near field, is presented. A description of the practical application and limitations of the method associated with ADCP measurements follows. Results of the estimates of SSC profiles at the field sites from the two different frequency BB-ADCPs are discussed and suggestions to improve the estimates are presented.

[1] Use of trade, product, or firm name is for descriptive purposes only and does not imply endorsement by the U.S. Geological Survey.

## 2. Acoustic method

The method of estimating mass concentration of suspended solids [$SSC_{(est)}$] from ABS employs a formula based on the sonar equation for sound scattering (reverberation) from small particles. In exponential form, the equation is

$$SSC_{(est)} = 10^{(A+B*RB)} \quad (1)$$

The exponent of Eq. (1) contains a term for the measured (e.g., by ADCP) relative acoustic backscatter, RB, as well as terms for an intercept, $A$, and slope, $B$, determined by regression of concurrent ABS with known mass concentration measurements ($SSC_{meas}$) on a semi-log plane in the form of $\log(SSC_{meas})=A+B*RB$. The relative backscatter is the sum of the echo level measured at the transducer plus the two-way transmission losses (Thevenot et al., 1992) as defined below.

### 2.1. Sonar equation

In its simplified form for reverberation, the sonar equation (Urick, 1975) can be written as

$$RL = SL - 2TL + TS \quad (2)$$

where RL is reverberation level, SL is the source level, which is the intensity of emitted signal that is known or measurable, 2TL is the two-way transmission loss, and TS is the target strength which is dependent on the ratio of wavelength to particle diameter. All variables are measured in dB. In terms of ADCP parameters, $RL=K_c(E-E_r)$, where $E$ is ADCP echo intensity recorded in counts, $E_r$ is ADCP received signal strength indicator (RSSI) reference level (the echo baseline when no signal is present), in counts, and $K_c$ is the RSSI scale factor used to convert counts to dB. $K_c$ varies among instruments and transducers and has a value of 0.35–0.55 (Deines, 1999). The two-way transmission loss, 2TL, is defined as

$$2TL = 20\log(R) + 2\alpha R \quad (3)$$

where $R$ is range to the ensonified volume, in meters, $\alpha$ is an absorption coefficient, in dB/m. $20\log(R)$ is the term for loss due to spreading and $2\alpha R$ is the term for loss due to absorption. The absorption coefficient for water is a function of acoustic frequency, salinity, temperature, and pressure (Schulkin and Marsh, 1962). The spreading loss is different in near and far transducer fields. The transition between near and far transducer fields is called the critical range, $R_{\text{critical}}$. $R_{\text{critical}}=\pi a_t^2/\lambda$, where $a_t$ is the transducer radius, in cm, and $\lambda$ is acoustic wavelength. The near-field correction, $\Psi$, for spreading loss is calculated from the formula in Downing et al. (1995) as

$$\Psi = \left[1 + 1.35Z + (2.5Z)^{3.2}\right] / \left[1.35Z + (2.5Z)^{3.2}\right] \tag{4}$$

where $Z$ is $R/R_{\text{critical}}$. $R_{\text{critical}}$ is 167 cm for a 1200-kHz ADCP with a 5.1-cm-diameter transducer and 80 cm for a 2400-kHz ADCP with a 2.5-cm-diameter transducer.

For the particle size range and acoustic frequencies of interest here, attenuation from suspended sediment consists of a viscous loss component and a scattering loss component (Flammer, 1962). In the presence of suspended sediments that are generally less than 100–200 μm, the viscous and scattering components of attenuation change in opposing ways to changes in size. Viscous losses go up as sediment size decreases and scattering losses go up as size increases. Scattering characteristics are a function of $\lambda$ to particle circumference $2\pi a_{\text{p}}$, where $a_{\text{p}}$ is particle radius. When $\lambda \gg 2\pi a_{\text{p}}$, the majority of the scattering pattern propagates backward; however, as $\lambda$ approaches $2\pi a_{\text{p}}$, the scattering pattern increases in complexity, and when $\lambda \ll 2\pi a_{\text{p}}$ half the scattered pattern propagates forward and the remainder is scattered through all directions (Flammer, 1962). In the case of a 1200 and 2400 kHz acoustic sources, $\lambda=2\pi a_{\text{p}}$ for 400- and 200-μm-diameter particle sizes, respectively. Using Flammer's (1962) equations, attenuation from particle scattering approaches that of the water alone when particle sizes approach about 125-μm diameter in concentrations approaching 1000 mg/l for a 2400-kHz ADCP.

Similar to scattering losses, viscous losses are frequency dependent; larger losses occur with higher frequencies. In the case of the 2400-kHz ADCP, attenuation from the viscous-loss component approaches that from water alone when particle sizes fall below about 10 μm in concentration levels of about 1000 mg/l.

Taken together, scattering- and viscous-loss terms account for little attenuation with 1200-kHz frequency unless particle size is very small or concentrations are very high. However, in the case of the 2400-kHz ADCP, total attenuation may need to be accounted for even at lower concentrations if particles are very small (viscous losses) or larger than about 100–150 μm diameter (scattering losses).

All these calculations assume solid spherical mono-size particles. Determination of attenuation in the presence of a log-normal particle size distribution would be more complex but unlikely to differ meaningfully from values presented here. However, attenuation losses from suspensions that are primarily composed of aggregated particles are unknown. Thorne et al. (1991) found that, in the case of 3.0- and 5.65-MHz acoustic frequencies, attenuation from fine sands may become significant at ranges on the order of a meter when concentration levels approach 100 mg/l. Therefore, attenuation due to presence of sediment is accounted for in this analysis in which mass concentrations encountered in the field study are generally in the range of 0–300 mg/l. Following Flammer (1962) a coefficient, $\zeta$ is defined as

$$\zeta = K(\gamma-1)^2\left\{S/\left[S^2+(\gamma+\tau)^2\right]\right\} + \left(K^4 a_{\text{p}}^3\right)/6 \tag{5}$$

where $K$ is $2\pi/\lambda$, $\gamma$ is the particle or aggregate wet density divided by the fluid density, $\tau$ is $0.5+9/(4\beta a_{\text{p}})$, $S$ is equal to $[9/(4\beta a_{\text{p}})][1+1/(\beta a_{\text{p}})]$, $\beta$ is equal to $[\omega/2v)]^{0.5}$, $\omega$ is $2\pi f$, $f$ is frequency in MHz, and $v$ is the kinematic viscosity of water, in stokes. The two-way attenuation from suspended particles, $2\alpha_{\text{s}}$ in dB/cm is equal to (8.68)($\zeta$)(SSC), where SSC is in ppm and 8.68 is the conversion from nepers to dB. The first term in Eq. (5) is the attenuation from viscous losses and the second term is the attenuation from scattering losses.

From a practical standpoint, it is not necessary to know the source level nor is it possible to measure all the characteristics of suspended material required to directly model target strength (Thevenot et al., 1992, Reichel and Nachtnebel, 1994). Therefore, following the derivation of Thevenot et al. (1992), Eq. (2) is cast in terms of relative backscatter, RB=RL+2TL. After appropriate substitutions, the sonar equation can be written in terms of concentration and relative backscatter as

$$\mathrm{SSC} = 10^{(-0.1K_2+0.1\mathrm{RB})} \tag{6}$$

where $K_2$ is a parameter that includes terms for source level, target strength, ensonified volume, and mass of suspended material. The theoretical parameters $A$=$-0.1K_2$ and $B$=0.1 are appropriate for a concentration of uniform particles of the same mass and other properties. For a distribution of particles in the field, agreement with the theoretical values is experimentally checked by regression of RB with measured estimate of total suspended solids concentration at the same location. Thevenot et al. (1992) determined the coefficient $-0.1K_2$ to be equal to 0.97 and 1.43 for laboratory and field calibrations, respectively. They determined values for the coefficient multiplying RB to be 0.077 (laboratory) and 0.042 (field). Thus, Eq. (6) can be used to estimate time series of SSC from ADCP ABS at any distance from the acoustic transducer where valid backscatter data are available once appropriate transmission losses and slope and intercept values are determined.

### 2.2. Application of technique to BB-ADCP data

Doppler profilers are commercially available instruments used to measure water motion using acoustic properties of sound transmitted at fixed frequency. The instrument measures phase or frequency change of echoes backscattered from suspended material (plankton and sediment) in the water and converts the echoes to along (acoustic) beam velocity components. The ADCP then converts the along beam velocities to north/south, east/west, and vertical velocity components. Velocity profiles are determined by a process called range gating (breaking the received signal into segments) so that velocities are determined at preset intervals along the acoustic path (called depth cells or bins). Velocity measurements with as little as 5-cm resolution (bin size) are possible with the Broadband version of the ADCP operating in certain high-resolution modes.

To estimate a time series of SSC from a time series of ADCP acoustic backscatter intensity, the following practical approach can be applied. First, determine the ADCP RSSI reference level, $E_r$, as a function of power and individual instrument. This can be accomplished by putting the ADCP transducer in clear water and determining the RSSI values (Deines, 1999) or by using results of one of the instrument built-in tests. Alternatively, the lowest backscatter measured during an observation sequence can be used as the baseline. Next, determine the absorption coefficient, $\alpha$, as a function of salinity, temperature, pressure, and ADCP frequency. Find the range of near/far field transition for the ADCP transducer, $R_{\mathrm{critical}}$, as a function of ADCP frequency and transducer diameter. Then, determine the slant range to each ADCP bin as a function of transducer angle, and other ADCP setup properties such as ADCP blank, bin size, and transmit pulse length, and the sound speed. (ADCP blank is a time delay expressed as distance from the transducer in which signal is unusable because of transducer ringing after a transmitted sound pulse.) Find the two-way transmission loss from spreading and absorption to/from each bin as a function of range and the absorption coefficient (Eq. (3)) including the near-field transducer correction (Eq. (4)) for spreading loss. The near-field correction is necessary because, in the instrument configuration used for these field tests, most of the sampled profile is within the near field of the ADCP transducers. Utilizing Eq. (5) and the mass concentration measured by OBS or water samples determine the attenuation from suspended material in the acoustic path. Then, determine relative backscatter, RB (in dB) at each bin for every profile by removing the RSSI reference level (or baseline), correcting for transmission losses and converting backscatter units to dB utilizing an RSSI scale factor. Once the relative backscatter is determined, calculate the $\log_{10}$ of the $\mathrm{SSC_{meas}}$ to be used for calibration. Finally, determine the slope and intercept for a regression between $\log_{10}(\mathrm{SSC_{meas}})$ and relative backscatter, RB, such that $\log_{10}(\mathrm{SSC_{meas}})=A+B(\mathrm{RB})$. New (estimated) time series of profiles of SSC can then be determined from ADCP backscatter profiles (corrected for transmission loss and RSSI reference level) at each bin level utilizing Eq. (1).

There are, however, two practical limitations to the method. The first is the common limitation of any single-frequency instrument (either optical or acoustic). Single-frequency instruments alone cannot differentiate between changes in concentration level and changes in particle size distribution. In short, if mass concentration remains constant but particle size distribution changes during a measurement period without additional calibrations, a single-frequency instrument will output a change in mass concentration. The amount of error depends on the type of instrument and the amount of change in size distribution. The second limitation depends on instrument frequency and particle size of the suspended material. As explained in the following section, this is typically not a limitation of optical sensors but must be considered when using acoustic sensors.

### 2.3. Acoustic frequency vs. particle size

Operating frequencies of acoustic instruments designed to measure velocity profiles are chosen based on required sampling ranges because signal attenuation (from the water as well as the suspended material) is highly correlated with frequency. High instrument frequencies result in short instrument ranges and vice versa. The result is that an instrument optimally designed to estimate velocity from acoustic backscatter may be an inefficient instrument for measuringsuspended sediment under some conditions.

As previously mentioned, one of the critical limitations of the ABS method to estimate SSC is the relation between particle size and acoustic frequency. The appropriate technique for estimating SSC from acoustic backscatter utilizes the Rayleigh scattering model that is restricted to $2\pi a_p/\lambda<1$ (Reichel and Nachtnebel, 1994). Because wave number $k=2\pi/\lambda$, then this limit can be written as $ka_p<1$, where $ka_p$ is a nondimensional frequency. For a 1200-kHz ADCP; $ka_p=1$ corresponds to a particle diameter of 400 μm. The corresponding diameter for a 2400-kHz ADCP is 200 μm. When the size of suspended material is sufficiently large that the value of $ka_p$ approaches unity, errors in value of estimated SSC begin to grow. In addition, the acoustic method for estimating SSC may be inappropriate if particle size distribution is too small (Lynch et al., 1994; Schaafsma et al., 1997). However, the presence of aggregated suspended solids in estuaries such as San Francisco Bay may provide "equivalent" particle size distributions in the range of applicability even if noncohesive particle size distribution is quite small. It is more important to note that the relationship of acoustic wavelength to particle size may require recalibration if particle size distribution changes.

## 3. Study area and methods

San Francisco Bay is a complex estuarine system comprising two hydrologically distinct subestuaries (Fig. 1): the northern reach, which connects the confluence of the San Joaquin and Sacramento Rivers with the Pacific Ocean at Golden Gate, and South San Francisco Bay (South Bay). The northern reach receives most of the freshwater that enters the bay system. South Bay is considered a semienclosed embayment that is generally vertically well-mixed except during periods of high local runoff and river discharge. Tides and tidal currents in the bay are mixed diurnal and semidiurnal types, mainly semidiurnal (Conomos et al., 1985).

As part of an ongoing research program to better understand bottom boundary layer properties and sediment transport, two sites were chosen for deployment of an instrument platform equipped with a variety of instruments to measure hydrodynamic and water quality characteristics in South Bay during October 1998. A suite of instruments including a 1200-kHz ADCP and a 2400-kHz ADCP was first deployed in the main channel just north of the San Mateo Bridge (SMB site) between October 19 and 23, 1998 (Fig. 1). The instruments were later moved to the main channel just south of the Dumbarton Bridge (DB site) between October 23 and 29, 1998. Water depths (relative to mean lower low water) were 16.1 m at the SMB site and 7.3 m at the DB site. The two locations shared similar hydrodynamic conditions; although spatial variability of bed sediments suggested that size distributions of suspended materials might be somewhat different at the two sites. Conomos (1963) found silt size fraction dominates the South Bay although the clay size fraction dominates in areas south of the San Mateo and Dumbarton Bridges. There is an area where the sand size fraction dominates north of the Dumbarton Bridge. Knebel et al. (1977) found that the modal diameter of suspended sediments ranged from 5 to 11 μm in South Bay.

In addition to the two ADCPs, the instrument platform contained four conductivity–temperature–depth (CTD) data loggers, four OBS sensors, and a LISST-100 (Laser In Situ Scattering and Transmissometry) (Fig. 2). The LISST-100 (see Pottsmith and Bhogal, 1995; Gartner et al., 2001), which is designed

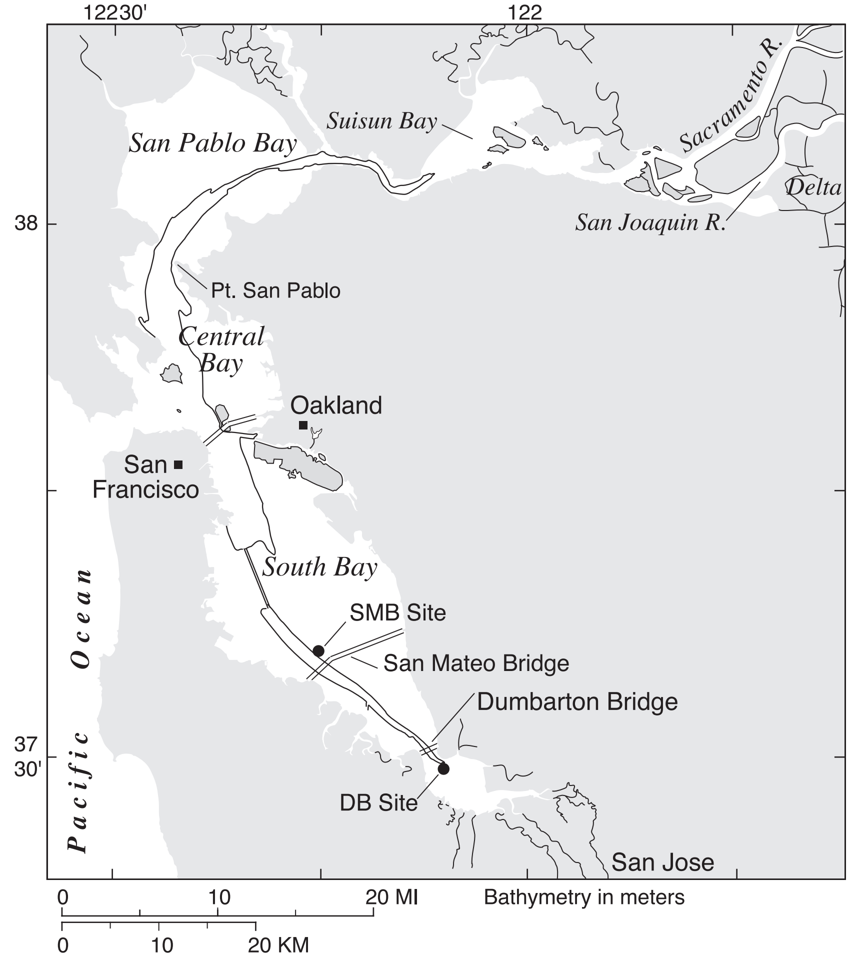


Fig. 1. San Francisco Bay estuarine system showing study sites at San Mateo Bridge (SMB) and Dumbarton Bridge (DB) in South San Francisco Bay, California.

for in situ measurement of particle size spectra and concentration as well as optical transmission, temperature, and pressure was mounted at 212 cm above bed. OBS sensors were mounted at 33, 63, 99, and 212 cm above bed; however, the data from the OBS mounted at 212 cm above bed were unusable because of problems with the data logger. CTDs were located at 33, 59, and 117 cm above bed.

Before instrument deployments, the OBSs were calibrated to estimate total mass concentration utilizing the upper few millimeters of bed material collected using grab samples at the two sites. Bottom sediment material was mixed with bay water in a large bucket and kept in suspension. The instruments were calibrated by taking measurements and water samples of suspended material in the bucket. Material in the bucket was successively diluted using surficial bay water to provide four concentration levels plus a sample of surface water only. These water samples were later filtered and weighed to determine actual sediment concentrations. Comparison of the instrument measured (voltage) and actual data forms a rating calibration curve for the OBSs.

The OBS measurements were recorded by the CTD data loggers. The CTD loggers recorded an average of 99 samples (taking less than 1 s for the 99 samples) once every 15 min during the field deployment. CTD data (conductivity, temperature, and pressure) were used to describe general hydrodynamic conditions and to determine the time series of attenuation coefficients

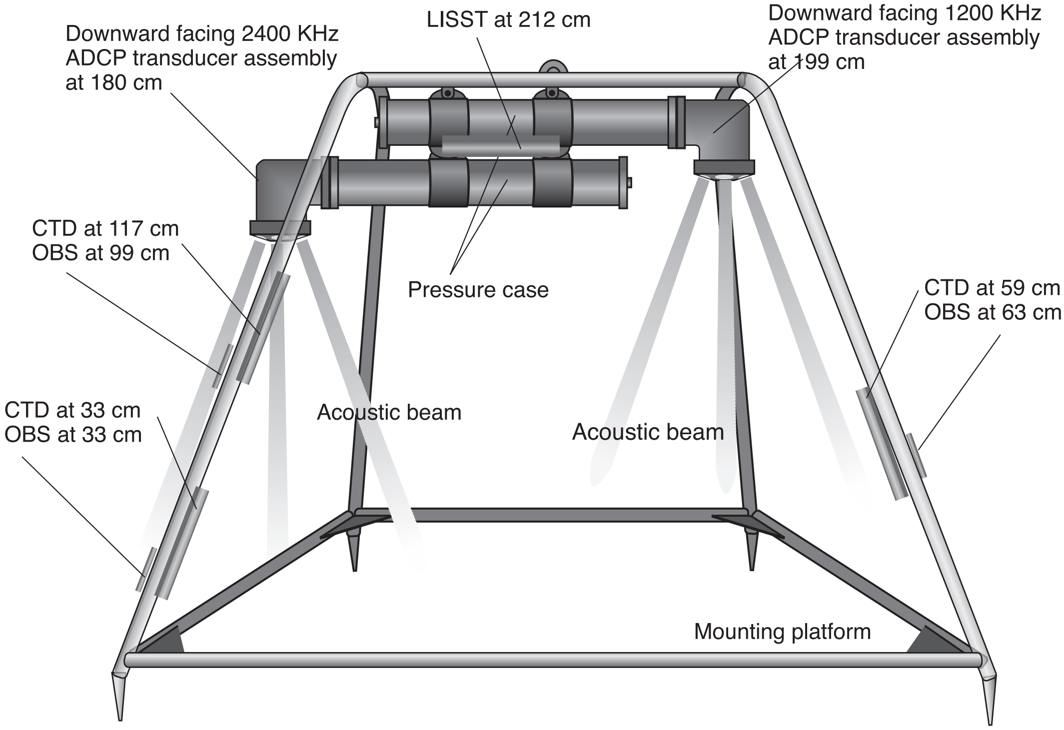


Fig. 2. Diagram of instrument mooring showing arrangement of 1200-kHz ADCP (transducer at 199 cm above bed) and 2400 kHz ADCP (transducer at 180 cm above bed) . OBS sensors were located at 33, 63, and 99 cm above bed and CTD sensors were located at 33, 59, and 117 cm above bed. The LISST-100 was located at 212 cm above bed.

for the transmission loss calculations in the SSC estimates.

The ADCPs were oriented in a downward configuration (Fig. 2); bin 1 of the 1200-kHz ADCP was at 128 cm above bed and bin 1 of the 2400-kHz ADCP was at 149 cm above bed. This resulted in most of the measurement profile falling within the transducer near field. Both ADCPs were programmed for 175 pings per ensemble with a 15-min sample interval between ensembles. Approximate time for the ensemble measurements was 18 s for the 1200-kHz unit and 16 s for the 2400-kHz unit. Both ADCPs used RD Instruments water profiling mode 1 (WM1) (RD Instruments, 1997). The 1200-kHz unit used a 25-cm bin size and a 35-cm blank; the 2400-kHz unit used a 10-cm bin size and a 15-cm blank.

The LISST-100 was used only for size distribution measurements during this study; unsuccessful calibration precluded use for estimates of total mass concentration The LISST-100 was programmed to record an average of 16 scans at about 4-Hz sampling rate once every 15 min.

General hydrodynamic conditions (as measured by the CTD at 117 cm above bed, the ADCP at 128 cm above bed, and the LISST at 212 cm above bed) at the SMB and DB sites from October 19 to 29, 1998, are shown in Fig. 3. This sample period covered from near spring tides to near neap tides during which the range of tides at both stations was about 250 cm (Fig. 3A). Tidal currents (Fig. 3B,C) were similar at the two locations; maximum current speeds were about 50–60 cm/s. The mean particle size of the suspended materials as measured at the sites by the LISST-100 is shown in Fig. 3D. However, the time series of mean particle size shown in Fig. 3D do not reflect the presence of bimodal size distributions or any information about the relative percentage of cohesive vs. noncohesive suspended sediments as previously described by Gartner et al. (2001). Variations in mean particle size provide an indication of the potential change to particle size distribution and resulting

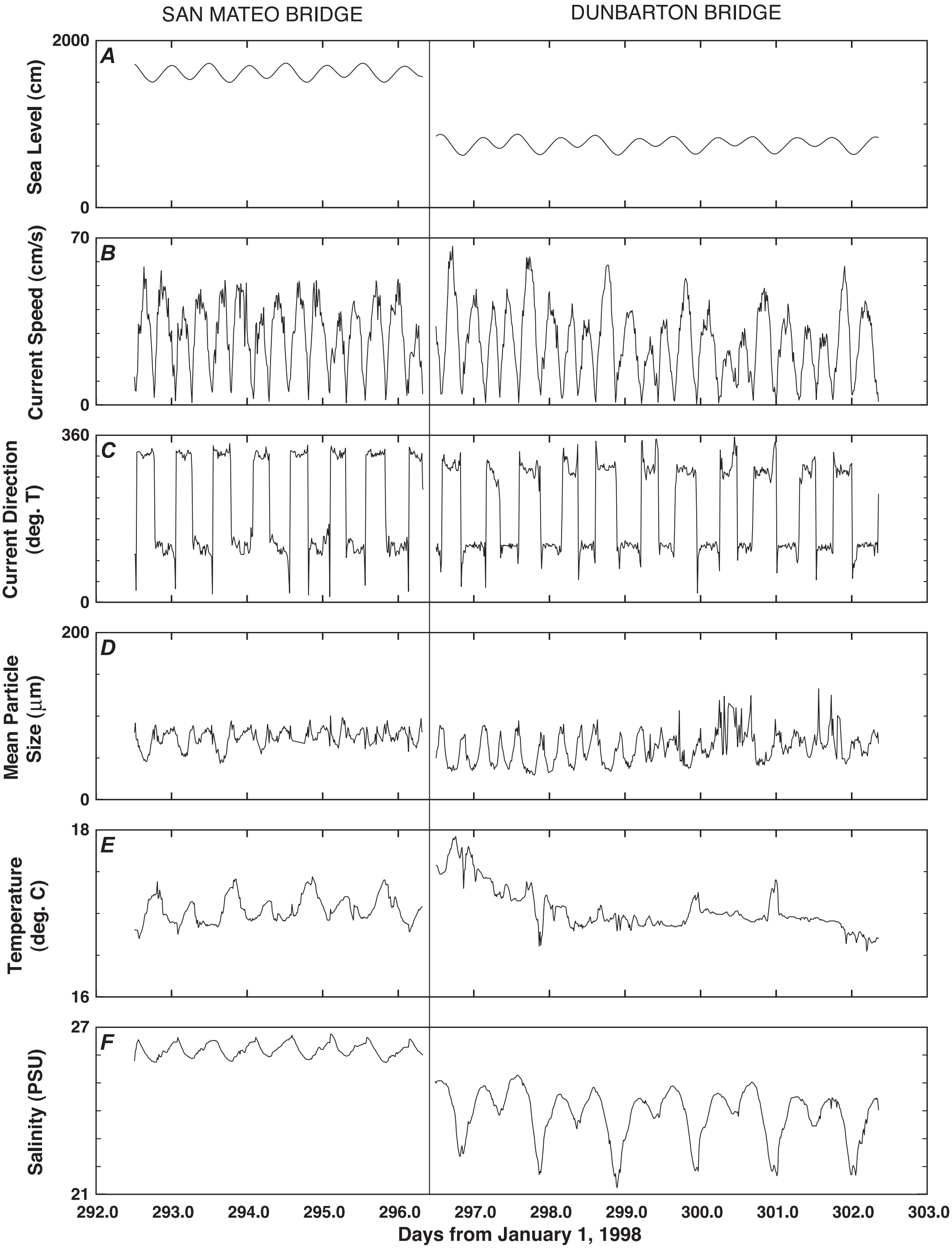


Fig. 3. Time series plots of hydrodynamic conditions at the San Mateo Bridge (day 292.5–296.4) and Dumbarton Bridge (day 296.5–302.3) showing water level (A), current speed (B), current direction (C), mean particle size (D), water temperature (E), and salinity (F). The vertical line near day 296.4 indicates break in record when instruments were moved from the SMB site to the DB site.

accuracy limitations of SSC estimates made from OBS and ADCP backscatter intensity measurements. Time series of temperature and salinity that were used with pressure to calculate a time series of the absorption coefficient for calculations are shown in Fig. 3E and F, respectively. Comparisons of top (117 cm above bed) and bottom (33 cm above bed) temperature and salinity records (not shown) indicate that the use of a single absorption coefficient to represent each profile was adequate. Top and bottom temperature values were essentially the same at both the DB and SMB sites as was salinity at the DB site. Salinity differences were less than about 0.1–0.2 PSU at the SMB site. Theoretically, changes of about 0.2 PSU at the temperatures and pressures found at the SMB site would produce errors less than 0.001 dB (0.1%) for transmission loss due to absorption.

Based on procedures outlined in Section 2.2, the following specific steps were applied in the present study to estimate a time series of profiles of suspended solids from ADCP backscatter intensity. The relative backscatter, RB (in dB), was determined progressively at each bin of every profile by removing the RSSI reference level, correcting for transmission loss from beam spreading and attenuation from water and sediment, and converting backscatter units to dB utilizing an RSSI scale factor (0.45 dB/count). New values for components of transmission loss to determine relative backscatter were calculated for every profile because new values for salinity, temperature, pressure, and SSC were available at the same sample interval and time as were the values of acoustic backscatter. The ADCP backscatter intensity used to calculate RB could be found from the average of backscatter measured by the four acoustic beams or the value from a single beam. In this case, results appear better if the average of multiple beams is used in calculations. Although RSSI scale factors other than 0.45 were tried, ultimately 0.45 was used in the calculations because the choice of alternative values could not be based on any physical characteristics, the original BB-ADCP receiver tests could not be located, and new receiver tests were not performed on the ADCPs because of operational considerations. Given the short distances to the bottom from the ADCP transducers (less than 2 m) and well-mixed water column at the experiment site, a time series of single values of $\alpha$ for each profile was used to represent the (water) absorption coefficient for the entire sample profile. Based on previous studies (Gartner et al., 2001), the value of 1.14 g cm$^{-3}$ was chosen for the aggregate wet density in Eq. (5) to correct for attenuation losses from suspended material. The SSC values used to correct for attenuation from suspended material were those measured by the OBS at 99 cm above bed. This approach provides a single value of attenuation for the profile; it does not account for changes in SSC that presumably increases near bottom. After calculating the $\log_{10}$ of the estimate of $SSC_{meas}$ from the OBS record closest to the ADCP transducer, the slope and intercept for a regression between $\log_{10}(SSC_{meas})$ and relative backscatter, RB, at the ADCP bin at the same location (1200-kHz ADCP bin 2 and 2400-kHz ADCP bin 6) were determined. (Obvious spurious data spikes resulting from fish or debris were removed from data sets before analysis.) For meaningful results, OBS estimates of less than 1 mg/l (if any) were reset to 1 mg/l before determining the $\log_{10}(SSC_{meas})$. New time series of profiles of SSC were estimated utilizing Eq. (1) and ADCP relative backscatter at each bin level. This process was repeated for the 1200- and 2400-kHz ADCPs at both the SMB and DB deployment sites.

## 4. Results

Evaluation of this technique of estimating suspended solids from backscatter intensity measured by commercially available ADCPs was performed by comparing the acoustic estimates with those made by OBS. Time series plots of SSC estimated from ADCP backscatter intensity and the OBS estimates at corresponding levels are shown in Figs. 4 and 5. (The time series for the lower OBS at 33 cm above bed is not compared with 1200-kHz ADCP data because acoustic backscatter from the corresponding ADCP bin was deemed invalid and unusable.) Because the acoustic calibration was performed using data from the upper OBS at 99 cm above bed corresponding with the 1200-kHz bin 2 and the 2400-kHz bin 6, the primary sources for evaluation of the technique are results at bin 4 of the 1200-kHz ADCP and bin 10 of the 2400-kHz ADCP that are compared to the middle OBS at 63 cm above bed.

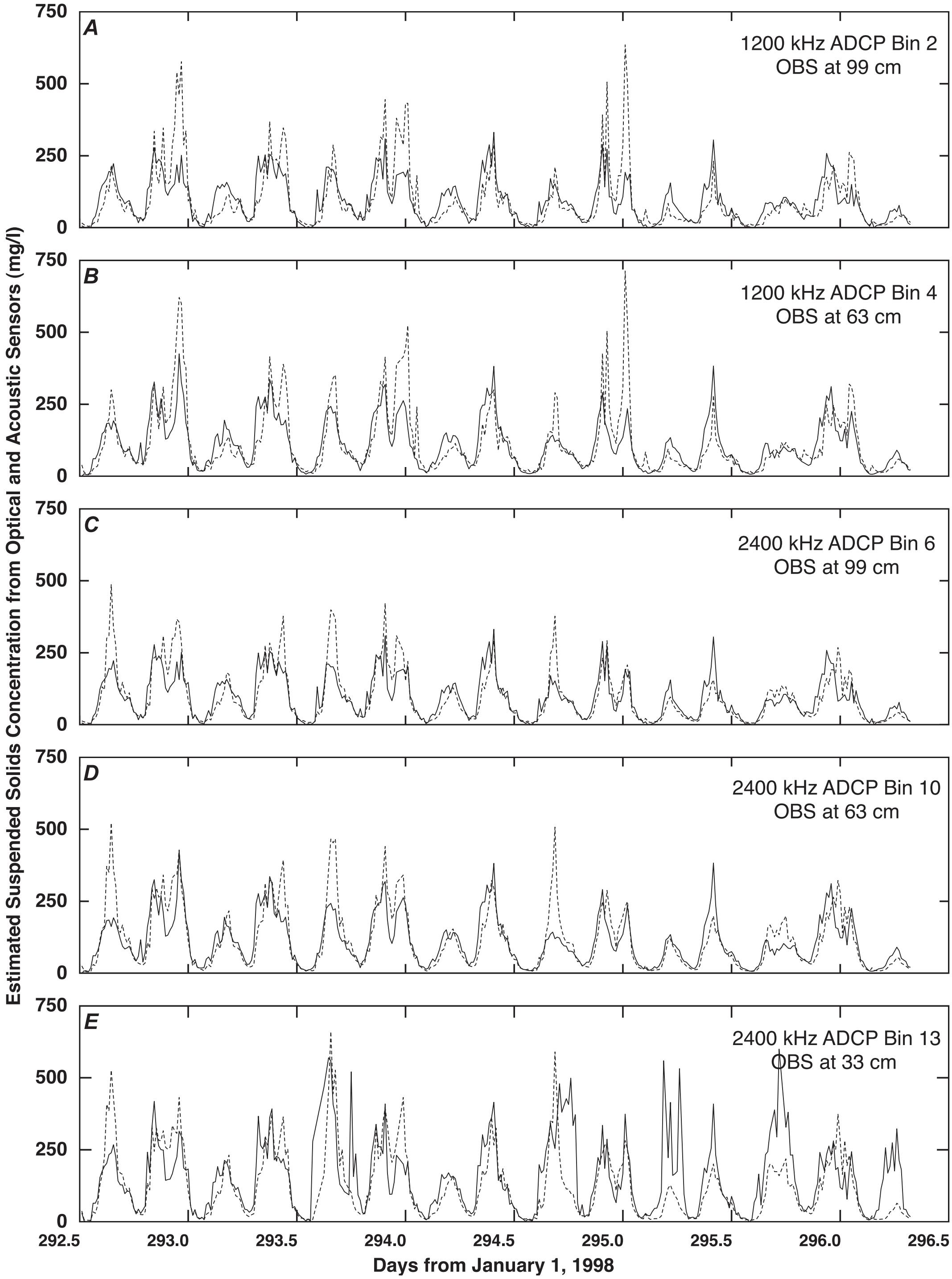


Fig. 4. Time series plots of comparisons between SSC estimated by OBS (solid lines) and SSC estimated by acoustic backscatter (dash lines) at the San Mateo Bridge site for the 1200-kHz ADCP (A) at bin 2, OBS 99 cm above bed and (B) at bin 4, OBS 63 cm above bed; and for the 2400-kHz ADCP (C) at bin 6, OBS 99 cm above bed, (D) at bin 10, OBS 63 cm above bed, and (E) at bin 13, OBS 33 cm above bed.

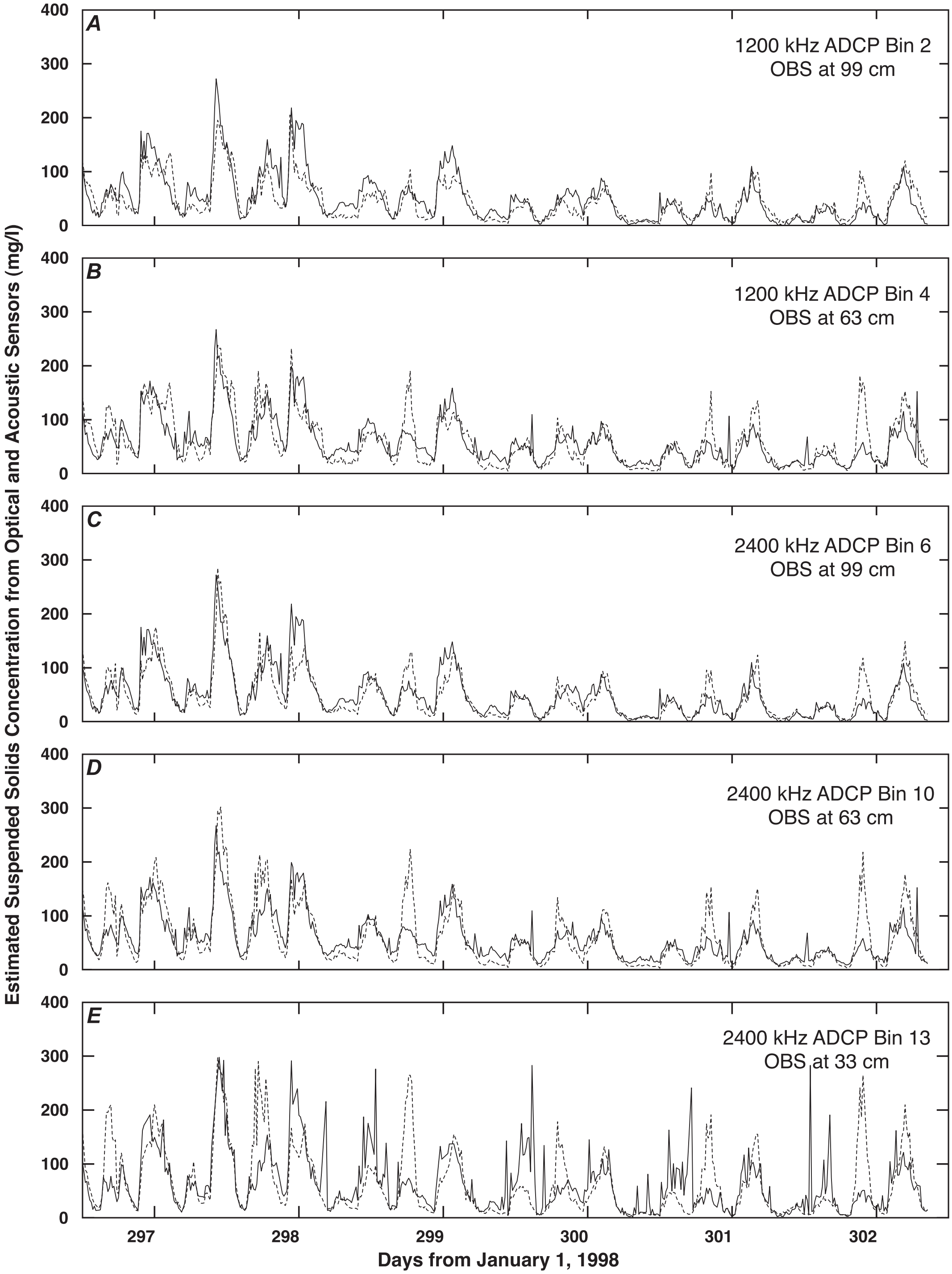


Fig. 5. Time series plots of comparisons between SSC estimated by OBS (solid lines) and SSC estimated by acoustic backscatter (dash lines) at the Dumbarton Bridge site for the 1200-kHz ADCP (A) at bin 2, OBS 99 cm above bed and (B) at bin 4, OBS 63 cm above bed; and for the 2400-kHz ADCP (C) at bin 6, OBS 99 cm above bed, (D) at bin 10, OBS 63 cm above bed, and (E) at bin 13, OBS 33 cm above bed.

However, it is also instructive to compare results at the top location to see how well the acoustic estimates match the optical estimates by which the acoustic backscatter was calibrated.

Figs. 4 and 5 show generally good qualitative agreement between the OBS estimates and the ADCP estimates although agreement between the 2400-kHz ADCP estimate at bin 13 and the bottom OBS located about 33 cm above bed appears poorer than at the middle or upper locations.

Statistical analyses were performed to quantify comparisons; results of those analyses are shown in Table 1. Average differences (in milligrams per liter) between the OBS and ADCP acoustic backscatter intensity estimates of SSC are shown in column 5. Those differences are shown as a percent relative to the range of estimated OBS concentrations (column 7) and the mean of estimated OBS concentrations (column 9). This is done to put the differences in perspective; for example, a 100% difference at 1 mg/l ($\pm$1 mg/l) is a far better result than a 10% difference at 1000 mg/l ($\pm$100 mg/l) by a factor of 2 orders of magnitude. Data spikes that were not obviously identified as spurious values to be removed before data processing have a large effect on the estimation statistics (see, for example, Fig. 4, near day 294.7, OBS at 63 cm).

Table 1 also shows the values for the slope and intercept that result from the regressions of $\log_{10}(SSC_{meas})$ and relative backscatter, RB. In the case of the October 1998 data sets, intercepts are generally small and the slopes close to 0.1, the theoretical value. Intercepts are nearly zero if the baseline (lowest) backscatter from the record is used in calculations of RB rather than the RSSI reference level. Regression results from two other data sets (SMB95 and SMB98) collected at different times at the San Mateo Bridge are shown in Table 1 for comparison. (SSC is estimated only at the regression point in the profiles because only one OBS data set was available during the SMB95 and SMB98 deployments.) Interestingly, the slopes from those regressions fall between about 0.04 to 0.05, a finding that suggests that the mean particle size or some other characteristic of the suspended material may have been different during February–March 1995 and July 1998 than during late October 1998. Unfortunately, no particle size data were determined during those field studies to help determine potential reasons for the slope differences.

Values in Table 1 show that regression results at the same location for different ADCP frequencies are closer than for the same instrument frequency at different locations (excluding SMB98 and SMB95). This indicates that for the 1200- and 2400-kHz ADCPs used here, spatial variations in suspended material (probably particle size distribution) is a more influential factor than instrument frequency for the size distributions seen at the SMB and DB sites during these deployments. This may be a result of

Table 1
Total suspended solids prediction statistics

| ADCP frequency (kHz) | OBS and ADCP bin location | Regression coefficients | | Difference (mg/l) | OBS range (mg/l) | Difference to OBS range (%) | OBS mean (mg/l) | Difference to OBS mean (%) |
|---|---|---|---|---|---|---|---|---|
| | | Slope | Intercept | | | | | |
| 1200 | SMB-TOP | 0.11492 | −6.24411 | 42.0 | 331.6 | 12.7 | 92.6 | 45.3 |
| 1200 | SMB-MID | | | 43.2 | 425.1 | 10.2 | 108.4 | 39.8 |
| 1200 | DB-TOP | 0.09274 | −4.34931 | 17.4 | 272.1 | 6.4 | 49.6 | 35.0 |
| 1200 | DB-MID | | | 20.1 | 260.7 | 7.9 | 58.2 | 35.3 |
| 2400 | SMB-TOP | 0.10943 | −4.46387 | 32.0 | 331.6 | 9.6 | 92.6 | 34.5 |
| 2400 | SMB-MID | | | 38.8 | 425.1 | 9.1 | 108.4 | 35.8 |
| 2400 | SMB-BOT | | | 63.1 | 599.4 | 10.5 | 149.4 | 42.2 |
| 2400 | DB-TOP | 0.08955 | −3.145 | 15.3 | 272.1 | 5.6 | 49.6 | 30.9 |
| 2400 | DB-MID | | | 22.0 | 260.7 | 8.4 | 58.2 | 37.8 |
| 2400 | DB-BOT | | | 33.1 | 296.0 | 11.2 | 60.8 | 54.8 |
| 1200 | SMB98 | 0.04933 | −0.74593 | 23.8 | 364.7 | 6.5 | 95.0 | 25.0 |
| 1200 | SMB95 | 0.04015 | −0.57666 | 9.3 | 598.2 | 1.6 | 36.6 | 25.5 |

Prediction difference is the difference in milligrams per liter between OBS estimate and ADCP acoustic backscatter estimate. Differences as percent are shown relative to the OBS estimated range of SSC (column 7) and OBS estimated mean of SSC (column 9).

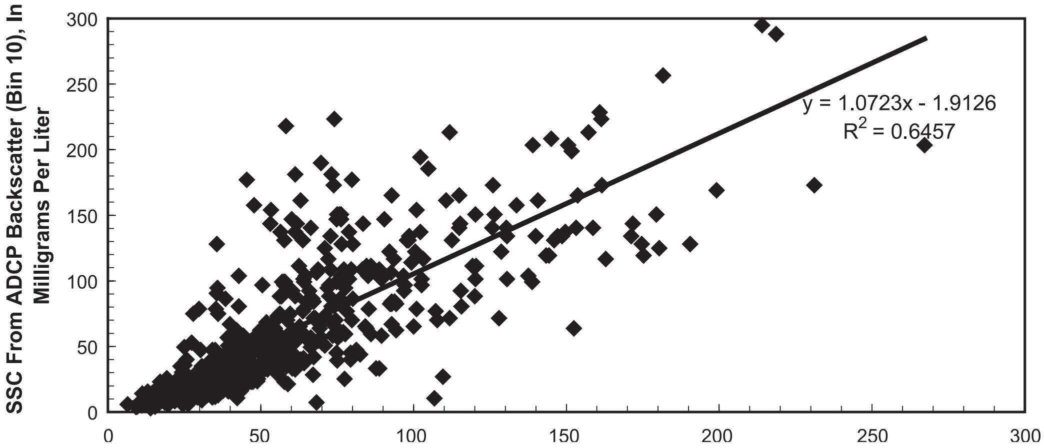


Fig. 6. Results of regression between estimates of suspended solids concentrations from OBS and ADCP backscatter at the Dumbarton Bridge at the middle OBS location (bin 10 of the 2400-kHz ADCP). The data trend line is shown.

the nature of the particles in suspension of which a large proportion are aggregates rather than single clay particles (Gartner et al., 2001) and thus less susceptible to limitations of the technique based on the frequency to size relation for very small particles. In any case, calibrations are site and time specific because, as with all single-frequency sensors, they are highly dependent on particle size distribution.

As an additional means of quantifying the differences between the two methods, scatter plots were constructed from the optical and acoustic estimates of SSC. One of those plots (2400-kHz ADCP bin 10, middle OBS at DB site) is shown in Fig. 6. Characteristics of the comparison trend lines of the scatter plots for all 10 data sets from October 1998 are shown in Table 2. Results shown in Table 2 indicate that the difference between OBS and ADCP estimates are larger near bed than at the middle and top location. In addition, the slope and intercept of the regression between optical and acoustic estimates of SSC at the top OBS location at the Dumbarton Bridge site varies substantially from 1.0 and 0.0, respectively, for both ADCP frequencies. However, the slopes of the trend lines approach 0.75 (1200 kHz) and 0.85 (2400 kHz) if the intercepts are forced through zero, as would be expected. $R^2$ values for all trend lines fall between about 0.30 (2400 kHz, Dumbarton Bridge, bottom) to 0.74 (2400 kHz, Dumbarton Bridge, top). Discounting the rather poor correlations for the two 2400-kHz ADCP estimations at the bottom location (33 cm above bed) and those at the top from which the

Table 2
Results of regressions between acoustic (ADCP) and optic (OBS) estimates of suspended solids concentrations

| ADCP frequency (kHz) | OBS and ADCP bin location | Regression slope | Regression intercept | $R^2$ | Regression slope | $R^2$ |
|---|---|---|---|---|---|---|
| 1200 | SMB-TOP | 1.054 | −3.3 | 0.543 | | |
| 1200 | SMB-MIDDLE | 1.071 | −0.5 | 0.604 | | |
| 1200 | DB-TOP | 0.679 | 10.9 | 0.707 | | |
| 1200 | DB-MIDDLE | 0.908 | 8.2 | 0.626 | | |
| 2400 | SMB-TOP | 1.046 | −1.5 | 0.678 | | |
| 2400 | SMB-MIDDLE | 1.039 | 3.2 | 0.653 | | |
| 2400 | SMB-BOTTOM | 0.635 | 28.1 | 0.438 | 0.746 | 0.415 |
| 2400 | DB-TOP | 0.826 | 6.5 | 0.736 | | |
| 2400 | DB-MIDDLE | 1.072 | −1.9 | 0.646 | | |
| 2400 | DB-BOTTOM | 0.634 | 23.3 | 0.292 | 0.853 | 0.230 |

Columns 6 and 7 show slope and $R^2$ values with regression line forced through zero for the two near-bed data sets.

calibrations were performed, the average $R^2$ value is about 0.63 for the four middle data sets.

As expected, estimates of SSC from both acoustic and optical techniques are highly correlated with current speed (graph not shown) with peaks in SSC occurring near maximum tidal currents and minimum values occurring near slack water. To examine the quality of OBS and ADCP estimates of SSC as a function of mass concentration and mean particle size, time series of estimates of SSC at the top location (99 cm above bed) are replotted along with the time series of mean size distribution (Figs. 7and 8). The two methods produce estimates of SSC that are generally closer at low mass concentrations than at high mass concentrations. Obvious differences between the OBS and ADCP estimates can be seen at about half of the peaks in concentration. In general, the optic technique (OBS) tends to overestimate and/or the acoustic method (ADCP) tends to underestimate SSC at times of smaller size distribution (as determined by LISST-100). These trends are reversed when the size distribution becomes larger. This is typical at the SMB site with a few exceptions where the 2400-kHz ADCP appears to overestimate SSC at times of smaller size distribution (Fig. 7; pts. 1–3). Similarly, at the DB site, the OBS tends to overestimate SSC (or the ADCP tends to underestimate SSC) when size distribution becomes smaller and like the SMB site, there are a few exceptions where the 1200- and 2400-kHz ADCPs appear to overestimate SSC (Fig. 8; pts. 1–3). Except for the few high estimates primarily from the 2400-kHz ADCP, these results appear consistent

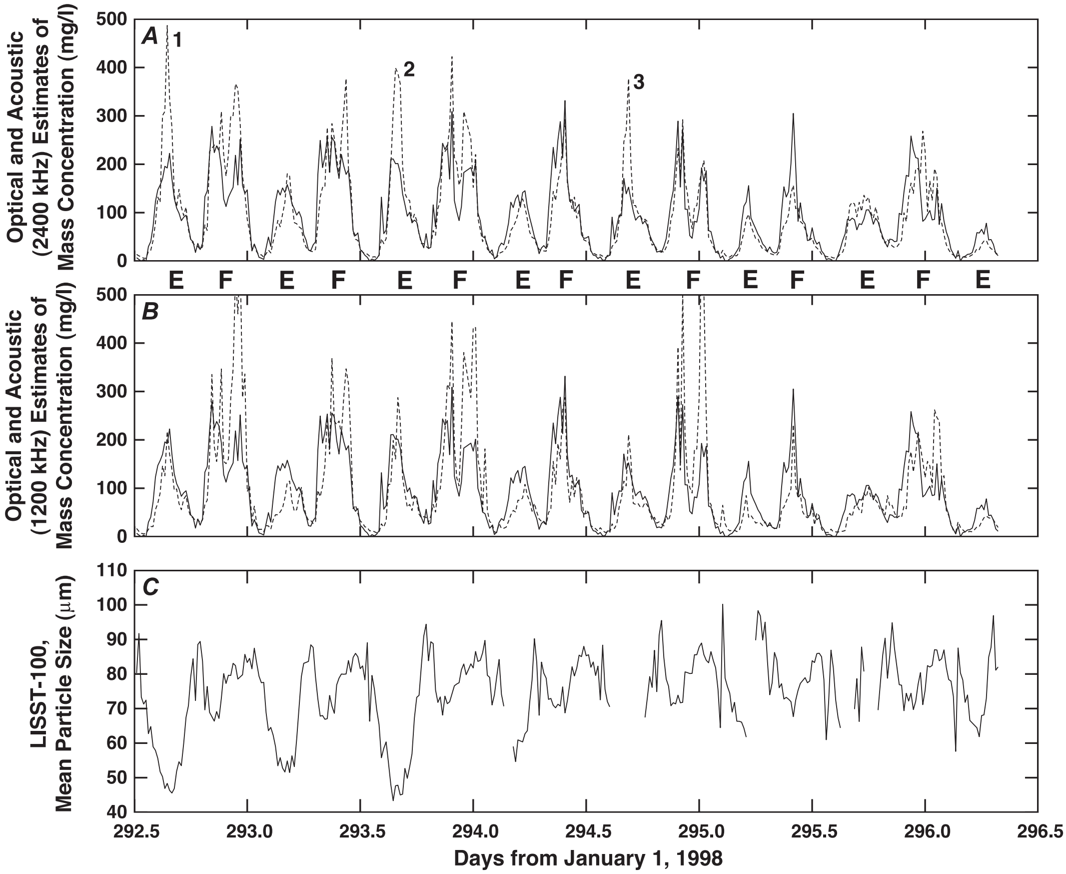


Fig. 7. Time series of estimated mass concentrations of suspended solids from (A); OBS (solid) and 2400-kHz ADCP backscatter (dash) at bin 6 (B); OBS (solid) and 1200-kHz ADCP backscatter (dash) at bin 2 (C); and mean particle size from LISST-100 at the San Mateo Bridge site. Es and Fs (between graphs A and B) show times of ebb and flood tides.

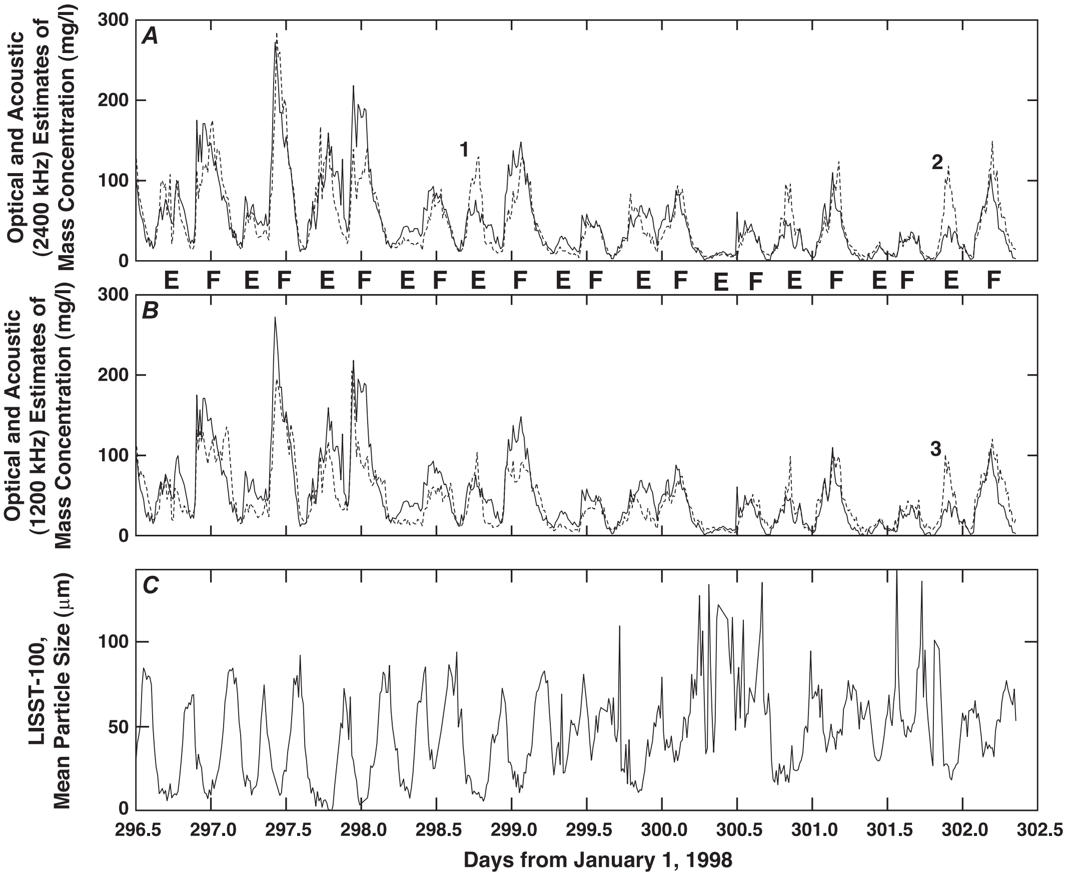


Fig. 8. Time series of estimated mass concentrations of suspended solids from (A) OBS (solid) and 2400-kHz ADCP backscatter (dash) at bin 6; and (B) OBS (solid) and 1200-kHz ADCP backscatter (dash) at bin 2; and (C) mean particle size from LISST-100 at the Dumbarton Bridge site. Es and Fs (between graphs A and B) show times of ebb and flood tides.

with theoretical characteristics of these methods; that is, optic sensors tend to overestimate, while acoustic sensors tend to underestimate, concentration when particle size distributions shift to a smaller size (and vice versa) (Lynch et al., 1994, Hamilton et al., 1998). Assuming for discussion that the OBS estimates are more correct, Fig. 7 shows a tendency for both ADCPs to overestimate SSC during flood currents and underestimate SSC during ebb currents at the SMB site. The ADCPs tend to underestimate SSC during flood currents at the DB site. These results differ somewhat from those of Holdaway et al. (1999) who found estimates by ADCP were generally lower than those by transmissometer during ebb current and generally agreed well during flood current. Jay et al. (1999) applied different calibrations to account for different size distributions during tidal cycles. They were unable to define any satisfactory calibration during one ebb current regime, suggesting local resuspension and advection played important and variable roles in producing a temporally varying size distribution (including large aggregate, sand, and silt). The variation in size distribution seen in the present study is somewhat narrower; Gartner et al. (2001) present measurements by LISST-100, indicating the fine silt and very fine sand fractions varied only about 5% at the SMB site and 5–10% at the DB site. However, in spite of similar calibration results, the 1200- and 2400-kHz ADCPs respond differently under some conditions, which points up the relation between frequency and particle size and one of the difficulties of calibrating acoustic backscatter.

One of the major advantages of the method of estimating SSC from profiles of acoustic backscatter

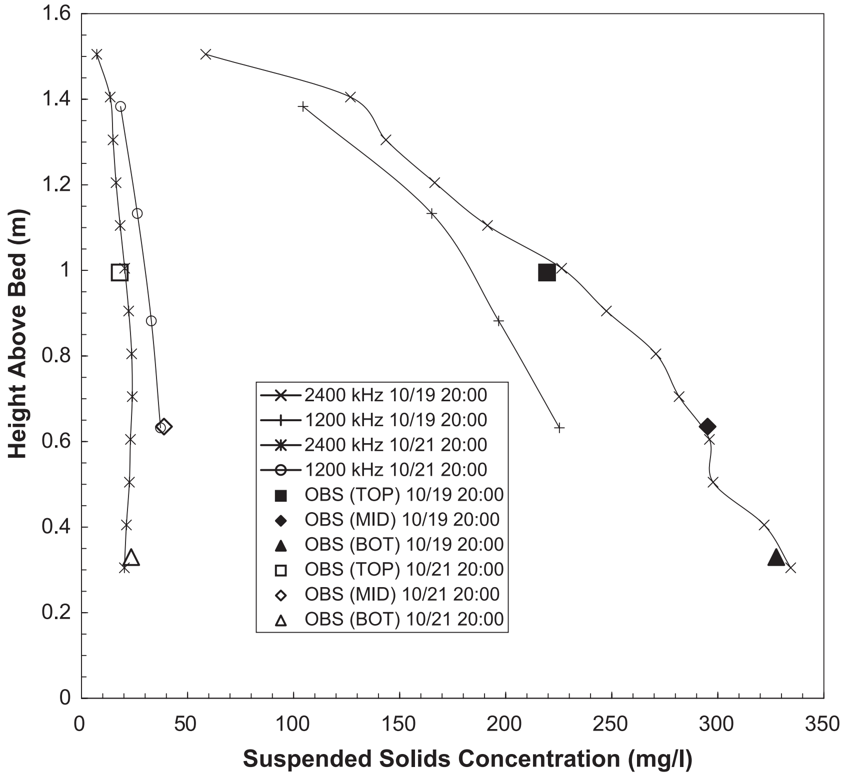


Fig. 9. Typical profiles of suspended solids concentration predicted from profiles of ADCP backscatter and OBS point measurements at 10/19/98 20:00 and 10/21/98 20:00. (Results shown are not meant to imply that the 1200-kHz ADCP backscatter produced results that were consistently lower than those from the 2400-kHz ADCP at high levels of SSC.

is the ability to estimate profiles of SSC. Examples of a few such typical profiles of SSC estimated from acoustic backscatter measured by 1200- and 2400-kHz ADCPs are displayed in Fig. 9. The estimated profiles of SSC are for times of both low and high mass concentration. (Although Fig. 9 shows the 1200-kHz ADCP underestimating SSC during one particular time of high SSC, it is not meant to imply that the 1200-kHz ADCP consistently underestimated values.)

## 5. Summary and conclusions

Estimates of SSC determined by commercially available ADCPs agreed favorably with those determined by OBS during field experiments in San Francisco Bay, California. Differences between OBS and ADCP estimates of SSC from the October 1998 data set at the middle OBS location varied from about 8% to 10% relative to OBS range and from about 35% to 40% relative to OBS mean. In general, the acoustic estimates compared less favorably to optic estimates near the bottom (2400 kHz) location. There are a number of possible factors to explain differences between optical and acoustic estimates. Those factors include (1) inaccuracies in the OBS estimates because of calibration errors; (2) an error in the RSSI scale factor used to convert ADCP backscatter intensity to dB; (3) errors in calculation of transmission losses at different distances from the transducers especially attenuation losses resulting from suspended solids materials; (4) errors in calculation of correction for the transducer near-field spreading losses; and (5) differences in sample average length for the OBS and ADCP.

It was expected that slopes for regressions between $\log_{10}(SSC_{meas})$ and relative backscatter, RB, would be similar for records from ADCPs with the same frequency at the same location with minor differences for records collected at different times (the result of temporal changes in particle size distribution). In fact, Table 1 shows remarkable consistency between regression slopes from the 1200- and 2400-kHz ADCP data at both stations. In addition, there are smaller than expected differences between regression slopes for the same frequency at the two sites. It is also interesting to note that regression slopes for the records collected at the San Mateo Bridge during different times are quite similar to each other (0.04–0.05) but different from those records from the 1200- and 2400-kHz ADCPs at SMB in October 1998 (0.11). This indicates that long-term temporal changes in SSC characteristics probably exceed spatial changes in the south end of South San Francisco Bay. Differences between optical and acoustic estimates of SSC at times of some maximum concentrations (currents) during the tidal cycle show a possible correlation with current direction and ADCP frequency. While changes in mean size distribution and percent fine silt and very fine sand remained small, some improvement in results is potentially possible with use of ebb/flood-dependent calibration data.

The short-term variability of suspended solids characteristics in San Francisco Bay points out the necessity of choosing a sample interval for OBS and ADCP backscatter measurements that is sufficiently short and sample and deployment lengths that are sufficiently long to provide a meaningful time series for analysis. Because of the high spatial and temporal variability of SSC, care must be taken to co-locate instruments and make recording at the same sample (mid) time. Different recording periods may be one of the major reasons for the differences between OBS and ADCP estimates in this study. Future efforts to estimate SSC from acoustic backscatter intensity must provide more nearly simultaneous recording by all instruments.

Inherent limitations to the technique based on the acoustic frequency relative to suspended particle size distribution is difficult to quantify and will always be an unknown source of error without independent information about particle size distribution. The method requires a reasonably steady size distribution of suspended material unless additional calibrations are performed. Additionally, because the acoustic backscatter intensity is calibrated from a time series of OBS estimates rather than analyzed water samples, possible errors in OBS calibrations (resulting from changes in particle size distribution or other characteristics that affect optical sensors) will affect the quality of the acoustic estimates. This is an inherent problem of a method designed to replace or supplement optical sensors or collected water samples, methods with their own limitations. To judge the accuracy of the method, one must depend, at least to some degree, on measurements and analyses techniques provided by traditional methods that the new method is designed to replace. Nevertheless, the presence of some cohesive material in estuaries may overcome limitations of the acoustic method in the areas of particle size and potential changes to size distribution, thus providing a very useful tool to make nonintrusive profiles of SSC concurrent with flow measurements using a commercially available instrument.

## Acknowledgements

The author acknowledges the many helpful and constructive comments of the anonymous reviewers.

## References

Buchanan, P.A., Schoellhamer, D.H., 1999. Summary of suspended-solids concentration data, San Francisco Bay, California, Water Year 1997. USGS OFR 99–189, 52 pp.

Conomos, T.J., 1963. Geologic Aspects of the Recent Sediments Of South San Francisco Bay, Master of Science Thesis San Jose State College, San Jose, CA, USA, 118 pp.

Conomos, T.J., Smith, R.E., Gartner, J.W., 1985. Environmental setting of San Francisco Bay. Hydrobiologia 129, 1–12.

Deines, K.L., 1999. Backscatter estimation using broadband acoustic Doppler current profilers. Proceedings of the IEEE Sixth Working Conference on Current Measurement, San Diego, CA, March 11–13, 1999, pp. 249–253.

Downing, A., Thorne, P.D., Vincent, C.E., 1995. Backscattering from a suspension in the near field of a piston transducer. Journal of the Acoustical Society of America 97 (3), 1614–1620.

Downing, J.P., Sternberg, R.W., Lister, C.R.B., 1981. New instrumentation for the investigation of sediment suspension processes in the shallow marine environment. Marine Geology (42), 19–34.

Downing, J.P., 1983. An optical instrument for monitoring suspended particles in ocean and laboratory. OCEANS 1983, San Francisco, California, August 29–September 1, 1983, Proceedings: pp 199–202.

Downing, J.P., 1996. Suspended sediment and turbidity measurements in streams: What they do and do not mean. Presented: Automatic Water Quality Monitoring Workshop, Richmond, B.C., February 12–13, 1996.

Flammer, G.H., 1962. Ultrasonic measurement of suspended sediment. U.S. Geological Survey Bulletin 1141-A. Government Printing Office, Washington, DC, p. 48.

Gartner, J.W., Cheng, R.T., Wang, P.F., Richter, K., 2001. Laboratory and field evaluations of the LISST-100 instrument for suspended particle size determinations, Marine Geology 175, pp. 199–219.

Hamilton, L.J., Shi, Z., Zhang, S.Y., 1998. Acoustic backscatter measurements of estuarine suspended cohesive sediment concentration profiles. Journal of Coastal Research 14 (4), 1213–1224.

Hammond, D.E., Fuller, C.C., Harmon, D.D., Hartman, Blayne, Korosec, Michael, Miller, L.G., Rea, Rebecca Warren, Stephen, Berelson William, Hager, S.W., 1985. Benthic fluxes in San Francisco Bay. Hydrobiologia 129, 69–90.

Hay, A.E., Sheng, Jinyu, 1992. Vertical profiles of suspended sand concentration and size from multi-frequency. Journal of Geophysical Research 97 (C10), 15,661–15,677.

Hill, D.C., Jones, S.E., Prandle, J., 2003. Derivation of sediment resuspension rates from acoustic backscatter time-series in tidal waters. Continental Shelf Research 23, 19–40.

Holdaway, G.P., Thorne, P.D., Flatt, David, Jones, S.E., Prandle, David, 1999. Comparison between ADCP and transmissometer measurements of suspended sediment concentration. Continental Shelf Research 19, 421–441.

Jay, D.A., Orton, Philip, Kay, D.J., Fain, Annika, Baptisa, A.M., 1999. Acoustic determination of sediment concentrations, settling velocities, horizontal transports and vertical fluxes in estuaries. Proceedings: 6th Working Conference on Current Measurement, 3/11–3/13, 1999, San Diego, CA, pp. 258–263.

Kuwabara, J.S., Chang, C.C.Y., Cloern, J.E., Fries, T.L., Davis, J.A., Luoma, S.N., 1989. Trace metal associations in the water column of South San Francisco Bay, California. Estuarine, Coastal and Shelf Science 28, 307–325.

Knebel, H.J., Conomos, T.J., Commeau, J.A., 1977. Clay–mineral variability in the suspended sediments of the San Francisco Bay system, California. Journal of Sedimentary Petrology 47, 229–236.

Land, J.M., Jones, P.D., 2001. Acoustic measurement of sediment flux in rivers and near-shore waters. Proceedings of the 7th Federal Interagency Sedimentation Conference, March 25–29, 2001, Reno, NV, pp. III 127–134.

Lynch, J.F., Irish, J.D., Sherwood, C.R., Agrawal, Y.C., 1994. Determining suspended sediment particle size information from acoustical and optical backscatter measurements. Continental Shelf Research 14 (10/11), 1139–1165.

Osborne, P.D., Vincent, C.E., Greenwood, B., 1994. Measurement of suspended sand concentrations in the nearshore: field intercomparison of optical and acoustic backscatter sensors. Continental Shelf Research 14 (2/3), 159–174.

Pottsmith, H.C., Bhogal, V.K., 1995. In situ particle size distribution in the aquatic environment. Presented at The 14th World Dredging Congress, Nov. 1995, Amsterdam, The Netherlands.

RD Instruments, 1997. DR/SC Acoustic Doppler Current Profiler: Technical Manual. RD Instruments, San Diego, CA, p. 380.

Reichel, G., Nachtnebel, H.P., 1994. Suspended sediment monitoring in a fluvial environment: advantages and limitations applying an acoustic Doppler current profiler. Water Research 28 (4), 751–761.

Schaafsma, A.J., Lafort, A.M., Guyomar, Daniel, 1997. Development of an acoustic method and prototype instrumentation for size and concentration measurement of suspended sediment. Proceedings of the First International Conference on EuroGOOS, 7–11 October, 1996. Elsevier, The Hague, The Netherlands, pp. 168–175.

Schulkin, M., Marsh, H.W., 1962. Sound absorptionin sea water. Journal of the Acoustical Society of America 34 (6), 864–865.

Thevenot, M.M., Kraus, N.C., 1993. Comparison of acoustical and optical measurements of suspended material in the Chesapeake Estuary. Journal of Marine Environmental Engineering 1, 65–79. Gordon and Breach Science Publishers.

Thevenot, M.M., Prickett, T.L., Kraus, N.C., 1992. Tylers Beach, Virginia, dredged material plume monitoring project 27 September to 4 October 1991. Dredging Research Program Technical Report DRP-92-7, US Army Corps of Engineers, Washington, DC, 204 pp.

Thorne, P.D., Vincent, C.E., Harcastle, P.J., Rehman, S., Pearson, N., 1991. Measuring suspended sediment concentrations using acoustic backscatter devices. Marine Geology 98. Elsevier, Amsterdam, pp. 7–16.

Urick, R.J., 1975. Principles of Underwater Sound, (2nd ed.). McGraw Hill, New York, p. 384.